Automatic Evaluation of Multi-Parameter Fluorescence Micrographs with a Neural Network Architecture

Tim W. Nattkemper,[1] Heiko Wersing,[1]
Walter Schubert,[2,3] Helge Ritter[1]

[1]Neuroinformatics Group, University of Bielefeld, P.O.-Box 10 01 31, D-33501 Bielefeld, Germany,
phone: +49 (0)521-106-6058, fax: +49 (0)521-106-6011,
email: {tnattkem,hwersing,helge}@techfak.uni-bielefeld.de
[2]Neuroimmunology and Molecular Pattern Recognition Research Group,
Institute of Medical Neurobiology University of Magdeburg
[3]MELTEC Ltd., University of Magdeburg,
phone: +49 (0)391-6117174, fax: +49 (0)391-6117176
email:schubert@pc.mdlink.de

Abstract

A neural network architecture for the automatic evaluation of fluorescence microscopy images of tissue samples is presented. One image is segmented into regions of fluorescent lymphocyte cell bodies and background. The system uses two kinds of neural nets to (i) detect the fluorescent cells and (ii) compute a one-pixel wide contour line for each detected cell. Even though the cells contours show considerable variation and the have non-homogenous fluorescence signals across the cell body the system detects a minimum of 95% of the cells with less than 10% false positives, using human expert evaluation of the images as a reference.

keywords: *shape recognition, contour grouping, fluorescence microscopy, functional proteomics*

1 Introduction

In this work we present a system for the rapid and exact evaluation of multi-parameter fluorescence images. The platform of our study is the evaluation of images of fluorescent lymphocytes in a tissue sample to prove the presence of n cell surface proteins at the cellular level simultaneously through immunofluorescence. The images are recorded by a special multi-parameter fluorescence microscopy technique, developed and standardized in the laboratory of one of the authors (W. S.) ([Schubert, 1992],[Schubert, 1997]) at the University of Magdeburg. The technique delivers n intensity images, referred to as *micrographs*, for one tissue sample and the existence of each protein at the cellular level is traced by the fluorescence of the cell in one image of the stack. Since the micrographs are generated by immunofluorescence, heterogenous signals, reflecting different concentrations of cell surface proteins, cause local distortions in the cells' fluorescence. Because the lymphocytes are located in tissue, their shapes show considerable variation and can be roughly characterized as *mainly convex*. Evaluation of the resulting, noisy images by human visual inspection is possible, but a highly tedious and very time-consuming task. Since the observers concentration decreases rapidly during the visual inspection the evaluation of the micrographs by human experts additionally is error-prone. This makes it necessary to develop computer vision algorithms for the automation of the micrograph evaluation. Computer vision algorithms in related applications are usually based on flooding schemes in gradient mountains [Meyer and Beucher, 1990], wave propagation [Hanahara and Hiyane, 1990], boundary tracing [Galbraith et al., 1991] or calculating saliency measures for groups of line segments combined with a backtracking algorithm [Jacobs, 1996]. A drawback of these algorithms is that they are based on defining a strict shape model for the objects in the image and an adaption to changes in scale and shape is a non-trivial task for a non-expert.
In the present work, we present an easy to train neural network architecture which (i) detects the fluorescent cells in every image of the stack and (ii) computes the cell contours for each detected cell. Careful visual inspection of the results by cytometric experts showed that the algorithm works with high precision in short computation time.

2 Multi-Parameter Fluorescence Imaging

To measure many quantitative cellular parameters of lymphocytes in liquid samples, high throughput screening (HTS) by flow cytometry has been shown to be a powerful technique for years. Flow cytometry is performed by the application of mono-clonal antibodies (mAbs) directed against cell surface antigens, referred to as the cluster of differentiation antigens (CD). Because the technique can only be applied to cells in liquids (blood) the analysis of immunoregulatory events were restricted to circulating cells.

In contrast to flow cytometry, cytometric measurements of lymphocytes in tissue so far largely remains restricted to time consuming and error-prone visual evaluation in various types of microscopes by human experts.
To identify cell surface proteins of lymphocytes in tissue we use fluorochrome antibody markers. Each marker binds to a subset of the lymphocytes in the sample which depends on the existence of the protein in the lymphocytes membrane. Fluorescence excitation makes the binding lymphocytes appear with high intensities and an image is taken by a CCD-camera. After that the process is repeated with another marker (see [Schubert, 1992],[Schubert, 1997] for details) until a stack of n images is recorded. During each repetition the positions of the lymphocytes are not affected, allowing a simultaneous measurement of cell surface proteins. To determine the protein information of one lymphocyte in the tissue sample the fluorescence intensities of the lymphocytes must be evaluated in all images of the stack.

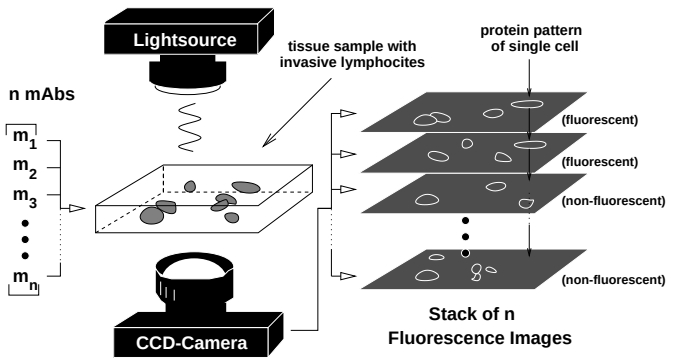

Figure 1: A sketch of the fluorescence microscopy imaging: The lymphocytes are prepared with n mAbs in an iterative procedure. At each step, the fluorescence excitation makes those lymphocytes appear in the image that bind to the mAb. An intensity image is taken by an integrated CCD-camera. After all n steps are completed a stack of n images with different subsets of fluorescent lymphocytes can be evaluated.

3 Automatic Evaluation of Fluorescence Micrographs

For the evaluation of one micrograph the fluorescent cells have to be detected and the contour of each detected cell has to be computed. The two evaluation steps are implemented by two modules. In the following, we can only provide a brief description of the modules. For details see the refererred publications.
The first module computes the positions of fluorescent cells in the image by calculating for each image pixel a probability measure, referred to as *evidence value*, that it is occupied by a fluorescent cell. The evidence values are computed by a pre-trained neural net of local linear map (LLM)-type [Ritter, 1991]. The LLM combines unsupervised and supervised learning in contrast to the widely used multi-layer perceptron trained with back-propagation [Rumelhart et al., 1986]. The training set of input/output-values for the LLM is computed from t image patches from one selected micrograph. One subset of the patches contains fluorescent cells, labeled by a biomedical expert using a computer mouse (fig. 2(1)), as positive training examples. The rest of the patches, the negative training examples, is built by randomly chosen patch centers in a minimum distance of five pixels to each of the patches from the positive example set. The training inputs for the LLM are 6-dimensional feature vectors $\mathbf{x}_\alpha, \alpha \in 1, \ldots, t$ computed from the image patches and argumented by the desired output value of $\mathbf{y}_\alpha = 1$, in case of a positive example and $\mathbf{y}_\alpha = 0$, else. The feature vectors are computed using 6 filter masks, that are eigenvectors (or *eigencells*) obtained from a principal component analysis (PCA) on the set of hand-selected (i. e., positive) cell patches (fig. 2(2)), which is an established technique in the field of Computer Vision (see [Turk and Pentland, 1991]). Thus, an image patch of $15 \times 15 = 225$ dimensions is projected to a 6-dimensional subspace, covering the most of the patch variance (fig. 2(3)). From the training set $\Gamma = \{(\mathbf{x}_\alpha, \mathbf{y}_\alpha)\}_{\alpha=1,\ldots,t}$ the LLM learns a mapping $C : \mathbb{R}^{d_{in}} \mapsto \mathbb{R}^{d_{out}} (d_{in} = 6, d_{out} = 1)$ by (i) a vector quantization of the input feature vector distribution (using a set of 5 reference vectors) and (ii) an adaption of local linear mappings into the output space, which are attached to each reference vector. The trained LLM-classificator performs the computation of the

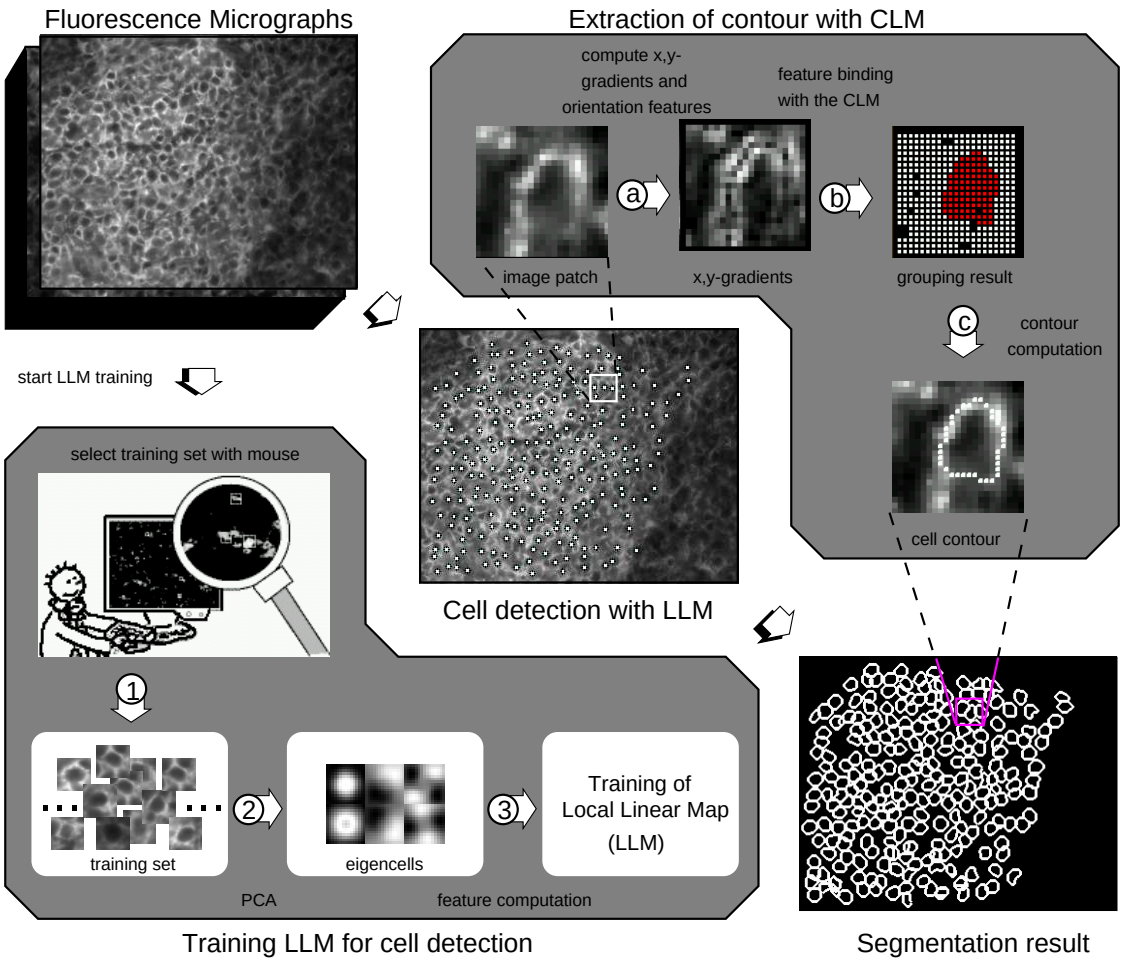

Figure 2: An illustration of the segmentation system. See the text for details.

evidence values (from the interval [0,1]) for image point features $\mathbf{x} \in \mathbb{R}^6$. Each evidence value is interpreted as a measure of belief that the point is occupied by a cell. The evidence values written to the corresponding image coordinates of the image point form a map of evidence values for the input image. High peaks in the evidence value mountains indicate a fluorescent cell at the corresponding position in the micrograph. A thresholding procedure combined with a local maximum search in the evidence map finally delivers the positions of fluorescent cells (white dots in the middle image in fig. 2). For a more detailed description, see [Nattkemper et al., 1999].

After the classification stage, a second processing stage attempts to determine for each detected fluorescent cell its precise boundary in the image. To this end, at each cell a 20×20-neighborhood is selected, so that it includes the whole cell body. The cell body is separated from its surrounding by grouping image primitives, referred to as features, to a salient mainly-convex group. The algorithm used to perform this grouping is a competitive layerered neural network (CLM) sketched briefly below and descripbed in [Ritter, 1990] and [Wersing and Ritter, 1999].

The features are the intensity x-,y-gradients of the neighborhood pixels, computed with sobel operators (fig. 2(a)). The grouping is achieved by dynamic feature binding only outlined in short here. The CLM consists of two layers of topographically organized nodes, each representing an edge feature in the input image neighborhood. Competitive and cooperative interactions between the features cause high activities of the cell-belonging nodes in the so called *figure* layer (grey dots in grouping result in fig.2) and low activities of the same nodes in the so called *ground* layer (white dots in grouping result in fig.2). For features belonging to the surrounding of the cell body the nodes behave vice versa. The dynamical integration of noisy local edge orientations into a coherent cell body group achieves a very precise and noise resistent segmentation

into cell body and background (fig. 2(b)).
Finally, using standard morphological operators [Sonka et al., 1993] a one pixel wide contour for the cell is computed easily (fig. 2(c)).

4 Results

Fluorescence micrographs of lymphocytes in tonsil tissue, recorded by our technique, were used for testing the performance of the system. The 658×517-sized micrographs show fluorescent cells so densely clustered, that they occlude each other partially. One segmentation result can be seen in the lower left corner in fig. 2. The accuracy of the segmentation was measured by taking the visual evaluation of the same set of images by a highly trained human expert as a reference. The system finds a minimum of 95% with a rate of false positives lower than 10%. The computation time for the image evaluation of about 250 cells less than 3 minutes on a Pentium II 450 MHz double processor machine.

5 Conclusion

We presented a system for the evaluation of fluorescence micrographs. The results were compared with the evaluation by a biomedical expert. It turned out that our approach works highly accurate. By the automation of the evaluation process, the system is free of influences such as fatigue and individual variance that affect human performance and the reproducibility of the human evaluation. In combination with the multi-parameter fluorescence microscopy technique the system provides a platform for the scalable extraction of simultaneous protein information of lymphocytes in many types of tissue.

Acknowledgments: This work was supported by DFG grant GK-231, Schu627/8-2, BMBF 07NBL04, BMBF 0311951, SFB 387 (TPB1).

References

[Galbraith et al., 1991] Galbraith, W., Wagner, M., Chao, J., Abaza, M., Ernst, L., Nederlof, M., Hartsock, R., Taylor, D., and Waggoner, A. (1991). Imaging cytometry by multiparameter fluorescence. *Cytometry*, 12:579–596.

[Hanahara and Hiyane, 1990] Hanahara, K. and Hiyane, M. (1990). A circle-detection algorithm simulating wave propagation. *Machine Vision and Applications*, 3:97–111.

[Jacobs, 1996] Jacobs, D. W. (1996). Robust and efficient detection of salient convex groups. *IEEE Trans. on Pattern Analysis and Machine Intelligence*, 18(1):23–37.

[Meyer and Beucher, 1990] Meyer, F. and Beucher, S. (1990). Morphological segmentation. *J. Visual Communications and Image Representation*, 1(1):21–46.

[Nattkemper et al., 1999] Nattkemper, T. W., Ritter, H., and Schubert, W. (1999). Extracting patterns of lymphocyte fluorescence from digital microscope images. In *Intelligent Data Analysis in Medicine and Pharmacology 99 (IDAMAP), Workshop Notes*, pages 79–88.

[Ritter, 1990] Ritter, H. (1990). A spatial approach to feature linking. In *Int. Neur. Netw. Conf. Proc. Paris*, volume 2, pages 898–901. Kluwer Publishers.

[Ritter, 1991] Ritter, H. (1991). Learning with the self-organizing map. In Kohonen, T., editor, *Artificial Neural Networks 1*. Elsevier Science Publishers, B.V.

[Rumelhart et al., 1986] Rumelhart, D., Hinton, G., and Williams, R. (1986). Learning internal representations by error propagation. *Parallel Distributed Processing: Explorations in the Microstructure of Cognition*, 1:Foundations:318–362.

[Schubert, 1992] Schubert, W. (1992). Antigenic determinants of t-lymphozyte $\alpha\beta$ receptor and other leucocyte surface proteins as differential markers of skeletal muscle regeneration: detection of spatially and timely restricted patterns by MAM microscopy. *Eur. J. Cell Biol.*, 58:395–410.

[Schubert, 1997] Schubert, W. (1997). Molecular semiotic structures in the cellular immune system: key to dynamics and spatial patterning? In J. Parisi, S.C. Mueller, W. Z., editor, *A perspective look at nonlinear media in physics, chemistry and biology, Lecture notes in physics.* Springer, Berlin.

[Sonka et al., 1993] Sonka, M., Hlavac, V., and Boyle, R. (1993). *Image Processing, Analysis and Machine Vision.* Chapman & Hall.

[Turk and Pentland, 1991] Turk, M. and Pentland, A. (1991). Eigenfaces for recognition. *Journal of Cognitive Neuroscience*, 3:71–86.

[Wersing and Ritter, 1999] Wersing, H. and Ritter, H. (1999). Feature binding and relaxation labeling with the competitive layer model. In *Proc. Eur. Symp. on Art. Neur. Netw. ESANN*, pages 295–300.